===================== **MATHEMATICAL MODELING** =====================

Analytical Study of Non-Newtonian Reiner – Rivlin Model for Blood Flow through Tapered Stenotic Artery

Nibedita Dash[*], Sarita Singh[**]

Department of Mathematics, School of Physical Sciences, Doon University, Dehradun, India

Abstract. Stenosis, the abnormal narrowing of artery, significantly affects dynamics of blood flow due to increasing resistance to flow of blood. Velocity of blood flow, arterial pressure distribution, wall shear stress and resistance impedance factors are altered at different degree of stenosis. Prior knowledge of flow parameters such as velocity, flow rate, pressure drop in diseased artery is acknowledged to be crucial for preventive and curative medical intervention. The present paper develops the solution of Navier – Stokes equations for conservation of mass and momentum for axis-symmetric steady state case considering constitutive relation for Reiner – Rivlin fluid. Reiner – Rivlin constitutive relation renders the conservation equations non-linear partial differential equations. Few semi-analytical and numerical solutions are found to be reported in literature but no analytical solution. This has motivated the present research to obtain a closed-form solution considering Reiner – Rivlin constitutive relation. Solution yields an expression for axial velocity, which is utilized to obtain pressure gradient, resistance impedance and wall shear stress by considering volumetric flow rate as initial condition. The effect of viscosity, cross viscosity, flow rate, taper angle of artery and degree of stenosis on axial velocity, resistance impedance and wall shear stress are studied.

Key words: artery, blood flow, cross viscosity, Reiner – Rivlin fluid, stenosis, viscosity.

INTRODUCTION

Cardiovascular diseases (CVDs), disorders of heart and blood vessels are the leading cause of death worldwide [1]. Usually death occurs because of heart attacks and strokes along with ischaemia, atherosclerosis and thrombosis. Heart attacks and strokes are acute events mainly caused by blockages, depriving heart and other vital organs of blood. Gradual accumulation of fatty deposits along the inner walls of the blood vessels restricts supply of blood and eventually blocks causing death. The abnormal narrowing of blood vessels in various locations of cardiovascular system due to the deposition of the cholesterol and other fatty substances leads to a medical condition called stenosis [2] causing a disorder called atherosclerosis. From etiological studies on stenosis, it is observed that deposition of calcium; fatty components and cholesterol on the inner walls of the artery prevent the flowing of blood leading to rupture of the artery and thrombosis, occluding the smaller vessels. The dynamics of blood flow is significantly affected in all these conditions. Stenosis increases the resistance to the flow of blood in arteries resulting in hypertension. It also induces substantial changes in velocity of blood flow, arterial pressure distribution, wall shear stress and resistance impedance. Prior knowledge of flow parameters such as velocity, flow rate, pressure drop in diseased artery is acknowledged to be crucial for preventive and curative medical intervention. Therefore, it is imperative to understand the behavior of blood flow in a stenotic artery that is significantly different from flow of blood in healthy artery.

---

[*]dashnibedita@yahoo.co.in
[**]saritamath@gmail.com

REVIEW OF LITERATURE

From the literature, it is revealed that many early attempts in modelling blood flow in a stenotic artery have considered Newtonian fluid property in basic Navier–Stoke's equations [3–6]. But, from various haemo-rheological experimentation [7–10], it is inferred that blood flow in artery exhibits non-Newtonian behaviour. Accordingly, researchers have considered three types of non-Newtonian blood properties: Thixotropy, visco-elasticity and shear thinning. Any of these three types of non-Newtonian model fails to describe the true rheological nature of blood flow [11–16]. Thixotropy and visco-elasticity, being transient property of blood, is exhibited at low shear rates and has a fairly long time scale. This suggests that thixotropy and visco-elasticity are of secondary importance in physiological blood flow [15]. Accordingly, researchers have considered different class of time independent fluid, usually exhibits shear thinning behaviour. The constitutive relation to account for apparent viscosity segregates into three zones. The lower Newtonian zone having low shear rate constant viscosity, upper Newtonian zone of high shear rate constant viscosity. In between there is a central zone of decreasing viscosity with increase in shear rate. Power law suitably explains this zone and fails to characterize the low and high shear rate zones. Herschel-Bulkley, Carreau, Casson, Cross model extends the power law model by including the yield stress in its expression. According to Tu and Deville [17], Sankar and Yatim [18], Tesch [19] and Verma [20] blood obeys as Casson fluid at moderate shear rate, whereas, Herschley-Bulkley fluid is applicable even for small shear rate. Further, Sankar and Yatim [18] have reported significant difference between the flow quantities and have concluded that use of Herschley-Bulkley fluid yields better results than Casson fluid in diseased artery. These models yield similar results in terms of wall shear stress at high shear rates but at low shear rate exhibits only qualitative similarity [21]. Besides shear rate, geometry and flow rate also influence the validity of fluid [21–23]. As diameter gets smaller Casson fluid fails to conform where as Herschley-Bulkley fluid continues to be valid [21, 22].

Fahraeus and Lindquist effect, where in blood viscosity depends on arterial diameter, is significant in stenosis as it constricts the artery in reducing its size. According to Hall [24] and Porenta [25], artery being long, narrow and slowly tapering cones, also affects the flow of blood. Considering the observation of Hall and Porenta, few models are reported those have considered tapered stenotic artery [26, 27]. Besides, Fahraeus – Lindquist effect and tapered artery, the effects of ratio of size of blood constituents to diameter of artery, deformability of blood constituents, including Merrington and Weissenberg effects are acknowledged to influence the flow characteristics of blood since blood is a suspension. Reiner – Rivlin fluid is reported to explain these complex physics [28–30]. The constitutive relation of Reiner – Rivlin fluid contains an extra term of cross viscosity. Therefore, consideration of Reiner – Rivlin fluid in developing blood flow model is expected to yield realistic results under conditions of blood flowing through tapered stenotic artery.

Reiner – Rivlin constitutive relation renders the conservation equations non-linear partial differential equations due to an extra term of cross viscosity with product of strain tensors. Few semi-analytical and numerical solutions are found to be reported in literature but analytical solution seems to be elusive due to mathematical complexity. This has motivated the present research to obtain a closed-form solution considering Reiner – Rivlin constitutive relation. Solution yields an expression for axial velocity, which is utilized to obtain pressure gradient, resistance impedance and wall shear stress by considering volumetric flow rate as initial condition. The effect of viscosity, cross viscosity, flow rate, taper angle of artery and degree of stenosis on axial velocity, resistance impedance and wall shear stress are studied.

PRELIMINARIES

Some preliminaries are presented here which will be used in sequel in formulating the problem for axi-symmetric case.

Constitutive equations for Reiner Rivlin fluid

Considering isotropic fluid, according to Reiner and Rivlin, the general relation between stress tensor τ_{ij} and rate of deformation ϵ_{ij} is given as:

$$\tau_{ij} = -p\hat{\delta}_{ij} + \mu\epsilon_{ij} + \mu_c\varepsilon_{ij},$$

where strain rate tensor $\varepsilon_{ij} = \epsilon_{ik}\epsilon_{kj}$, Kronecker delta $\hat{\delta}_{ij} = 1$ for $i = j$; $\hat{\delta}_{ij} = 0$ for $i \neq j$.

The stress tensors in cylindrical-polar coordinates (r, θ, z) are [29, 30]:

$$\tau_{rr} = -p\hat{\delta}_{rr} + \mu\epsilon_{rr} + \mu_c\left(\epsilon_{rr}\epsilon_{rr} + \epsilon_{r\theta}\epsilon_{r\theta} + \epsilon_{\theta z}\epsilon_{\theta z}\right); \text{ where } \hat{\delta}_{rr} = 1$$

$$\Rightarrow \tau_{rr} = -p + 2\mu\frac{\partial u}{\partial r} + \mu_c\left[4\left(\frac{\partial u}{\partial r}\right)^2 + \left(\frac{1}{r}\frac{\partial u}{\partial \theta} - \frac{v}{r} + \frac{\partial v}{\partial r}\right)^2 + \left(\frac{\partial v}{\partial z} + \frac{1}{r}\frac{\partial w}{\partial \theta}\right)^2\right],$$

$$\tau_{\theta\theta} = -p\hat{\delta}_{\theta\theta} + \mu\epsilon_{\theta\theta} + \mu_c\left(\epsilon_{\theta\theta}\epsilon_{\theta\theta} + \epsilon_{r\theta}\epsilon_{r\theta} + \epsilon_{\theta z}\epsilon_{\theta z}\right); \text{where } \hat{\delta}_{\theta\theta} = 1$$

$$\Rightarrow \tau_{\theta\theta} = -p + 2\mu\left(\frac{1}{r}\frac{\partial v}{\partial \theta} + \frac{u}{r}\right) + \mu_c\left[4\left(\frac{1}{r}\frac{\partial v}{\partial \theta} + \frac{u}{r}\right)^2 + \left(\frac{1}{r}\frac{\partial u}{\partial \theta} - \frac{v}{r} + \frac{\partial v}{\partial r}\right)^2 + \left(\frac{\partial v}{\partial z} + \frac{1}{r}\frac{\partial w}{\partial \theta}\right)^2\right],$$

$$\tau_{zz} = -p\hat{\delta}_{zz} + \mu\epsilon_{zz} + \mu_c\left(\epsilon_{zz}\epsilon_{zz} + \epsilon_{zr}\epsilon_{zr} + \epsilon_{\theta z}\epsilon_{\theta z}\right); \text{where } \hat{\delta}_{zz} = 1$$

$$\Rightarrow \tau_{zz} = -p + 2\mu\frac{\partial w}{\partial z} + \mu_c\left[4\left(\frac{\partial w}{\partial z}\right)^2 + \left(\frac{\partial u}{\partial z} + \frac{\partial w}{\partial r}\right)^2 + \left(\frac{\partial v}{\partial z} + \frac{1}{r}\frac{\partial w}{\partial \theta}\right)^2\right],$$

$$\tau_{r\theta} = \tau_{\theta r} = -p\hat{\delta}_{r\theta} + \mu\epsilon_{r\theta} + \mu_c\left(\epsilon_{rr}\epsilon_{r\theta} + \epsilon_{r\theta}\epsilon_{\theta\theta} + \epsilon_{zr}\epsilon_{\theta z}\right) \quad ; \text{ where } \hat{\delta}_{r\theta} = 0$$

$$\Rightarrow \tau_{r\theta} = \mu\left(\frac{1}{r}\frac{\partial u}{\partial \theta} - \frac{v}{r} + \frac{\partial v}{\partial r}\right) + \mu_c\left[\begin{array}{c}2\left(\frac{\partial u}{\partial r}\right)\left(\frac{1}{r}\frac{\partial u}{\partial \theta} - \frac{v}{r} + \frac{\partial v}{\partial r}\right) + 2\left(\frac{1}{r}\frac{\partial u}{\partial \theta} - \frac{v}{r} + \frac{\partial v}{\partial r}\right) \\ \left(\frac{1}{r}\frac{\partial v}{\partial \theta} + \frac{u}{r}\right) + \left(\frac{\partial u}{\partial z} + \frac{\partial w}{\partial r}\right)\left(\frac{\partial v}{\partial z} + \frac{1}{r}\frac{\partial w}{\partial \theta}\right)\end{array}\right],$$

$$\tau_{\theta z} = \tau_{z\theta} = -p\hat{\delta}_{\theta z} + \mu\epsilon_{\theta z} + \mu_c\left(\epsilon_{\theta\theta}\epsilon_{\theta z} + \epsilon_{\theta z}\epsilon_{zz} + \epsilon_{r\theta}\epsilon_{rz}\right); \text{ where } \hat{\delta}_{\theta z} = 0$$

$$\Rightarrow \tau_{\theta z} = \mu\left(\frac{\partial v}{\partial z} + \frac{1}{r}\frac{\partial w}{\partial \theta}\right) + \mu_c\left[\begin{array}{c}\left(\frac{1}{r}\frac{\partial v}{\partial \theta} + \frac{u}{r}\right)\left(\frac{\partial v}{\partial z} + \frac{1}{r}\frac{\partial w}{\partial \theta}\right) + 2\left(\frac{\partial v}{\partial z} + \frac{1}{r}\frac{\partial w}{\partial \theta}\right)\left(\frac{\partial w}{\partial z}\right) \\ + \left(\frac{1}{r}\frac{\partial u}{\partial \theta} - \frac{v}{r} + \frac{\partial v}{\partial r}\right)\left(\frac{\partial u}{\partial z} + \frac{\partial w}{\partial r}\right)\end{array}\right],$$

$$\tau_{rz} = \tau_{zr} = -p\delta_{rz} + \mu\epsilon_{rz} + \mu_c\left(\epsilon_{rr}\epsilon_{rz} + \epsilon_{rz}\epsilon_{zz} + \epsilon_{\theta z}\epsilon_{\theta r}\right); \text{ where } \hat{\delta}_{rz} = 0$$

$$\Rightarrow \tau_{rz} = \mu\left(\frac{\partial u}{\partial z} + \frac{\partial w}{\partial r}\right) + \mu_c\left[\begin{array}{c}2\left(\frac{\partial u}{\partial r}\right)\left(\frac{\partial u}{\partial z} + \frac{\partial w}{\partial r}\right) + 2\left(\frac{\partial u}{\partial z} + \frac{\partial w}{\partial r}\right)\left(\frac{\partial w}{\partial z}\right) \\ + \left(\frac{\partial v}{\partial z} + \frac{1}{r}\frac{\partial w}{\partial \theta}\right)\left(\frac{1}{r}\frac{\partial u}{\partial \theta} - \frac{v}{r} + \frac{\partial v}{\partial r}\right)\end{array}\right],$$

where, *u*, *v* and *w* are velocity vectors in radial, angular and axial directions respectively. Above generalized equations are used in formulating the present problem.

FORMULATION OF PROBLEM

The present paper attempts to solve Navier – Stokes equations for momenta and mass for axis-symmetric case considering constitutive relation for Reiner – Rivlin fluid. The model for blood flow in artery is formulated and subsequently the solution is obtained by considering following conditions.

297

i. If (r,θ,z) be the cylindrical-polar coordinate system with $r=0$ is the axis of symmetry of artery, the cylindrical co-ordinate (r,z) is considered where, $\dfrac{\partial}{\partial\theta}=0$.

ii. Flow of blood in artery is considered as incompressible Reiner – Rivlin fluid, i.e. $\left(\dfrac{\partial\rho}{\partial t}\right)=\left(\dfrac{\partial\rho}{\partial r}\right)=\left(\dfrac{\partial\rho}{\partial z}\right)=0$.

iii. Steady flow of blood is considered. Thus, $\dfrac{\partial}{\partial t}=0$.

iv. Viscosity is considered to be constant.

v. Density of blood is assumed to be constant.

vi. Radial component of velocity (u) is considered very small and considered to remain constant, ie. $\dfrac{\partial u}{\partial r}=0$.

Considering above conditions, the conservation equations in dimensional form are expressed as:

$$\frac{\partial\bar{u}}{\partial\bar{r}}+\frac{\bar{u}}{\bar{r}}+\frac{\partial\bar{w}}{\partial\bar{z}}=0$$

$$\rho\left(\bar{u}\frac{\partial\bar{u}}{\partial\bar{r}}+\bar{w}\frac{\partial\bar{u}}{\partial\bar{z}}\right)=\frac{1}{\bar{r}}\frac{\partial}{\partial\bar{r}}\left(\bar{r}\,\bar{\tau}_{\bar{r}\bar{r}}\right)+\frac{\partial\bar{\tau}_{\bar{z}\bar{r}}}{\partial\bar{z}}-\frac{\bar{\tau}_{\theta\theta}}{\bar{r}}$$

$$\rho\left(\bar{u}\frac{\partial\bar{w}}{\partial\bar{r}}+\bar{w}\frac{\partial\bar{w}}{\partial\bar{z}}\right)=\frac{1}{\bar{r}}\frac{\partial}{\partial\bar{r}}\left(\bar{r}\,\bar{\tau}_{\bar{z}\bar{r}}\right)+\frac{\partial\bar{\tau}_{\bar{z}\bar{z}}}{\partial\bar{z}}$$

Applying conditions considered in the paper, stress tensors in dimensional form for Reiner – Rivlin fluid reduces to

$$\bar{\tau}_{\bar{r}\bar{r}}=-\bar{p}+2\mu\frac{\partial\bar{u}}{\partial\bar{r}}+4\mu_c\left(\frac{\partial\bar{u}}{\partial\bar{r}}\right)^2,\ \ \bar{\tau}_{\theta\theta}=-\bar{p}+2\mu\frac{\bar{u}}{\bar{r}}+4\mu_c\left(\frac{\bar{u}}{\bar{r}}\right)^2,\ \ \bar{\tau}_{\bar{r}\theta}=0,\ \ \bar{\tau}_{\theta\bar{z}}=0,$$

$$\bar{\tau}_{\bar{r}\bar{z}}=\mu\left(\frac{\partial\bar{w}}{\partial\bar{r}}\right)+2\mu_c\left[\left(\frac{\partial\bar{u}}{\partial\bar{r}}\right)\left(\frac{\partial\bar{u}}{\partial\bar{z}}+\frac{\partial\bar{w}}{\partial\bar{r}}\right)+\left(\frac{\partial\bar{u}}{\partial\bar{z}}+\frac{\partial\bar{w}}{\partial\bar{r}}\right)\left(\frac{\partial\bar{w}}{\partial\bar{z}}\right)\right].$$

For the clarity, it is stated that $\bar{\tau}_{ij}$ represent dimensional form. All variables with superscript dash represent dimensional form and without dash as superscript represent non-dimensional form for the same variables.

These expressions are utilized to formulate the model for blood flow in artery considering blood as Reiner – Rivlin fluid. The schematic diagram of stenotic artery with coordinate system is shown in Fig. 1.

Let the following non-dimensional variables are introduced:

$$\bar{r}=rd_0\ ;\ \bar{z}=bz\ ;\ \bar{w}=u_0 w\ ;\ \bar{u}=\left(\frac{u_0\delta}{b}\right)u\ ;\ \bar{p}=\left(\frac{u_0 b\mu}{d_0^2}\right)p\ ;\ \bar{h}=d_0 h_z\ ;\ Re=\frac{\rho b u_0}{\mu}\ ;\ \gamma=\frac{\mu_c u_0}{\mu b}$$

$$\bar{\tau}_{\bar{r}\bar{r}}=\left(\frac{b}{u_0\mu}\right)\tau_{\bar{r}\bar{r}}\ ;\ \bar{\tau}_{\bar{z}r}=\left(\frac{d_0}{u_0\mu}\right)\tau_{\bar{z}r}\ ;\ \bar{\tau}_{\bar{z}\bar{z}}=\left(\frac{b}{u_0\mu}\right)\tau_{\bar{z}\bar{z}}\ ;\ \bar{\tau}_{\theta\theta}=\left(\frac{b}{u_0\mu}\right)\tau_{\theta\theta}\ .$$

The geometry of stenosis in non-dimensional form is described as [27, 28]:

$$h_z=\begin{cases} d_z\left[1-\omega\{(z-s)-(z-s)^n\}\right], \text{if } s\le z\le 1+s \\ d_z, \text{if otherwise}\end{cases},\qquad (1)$$

where $d_z = 1 + \varphi z$, $\omega = \dfrac{\delta (n)^{\frac{n}{n-1}}}{(n-1) d_0 b^n}$, $s = \dfrac{a}{b}$, n is shape factor and $\varphi = \tan \tilde{\theta}$.
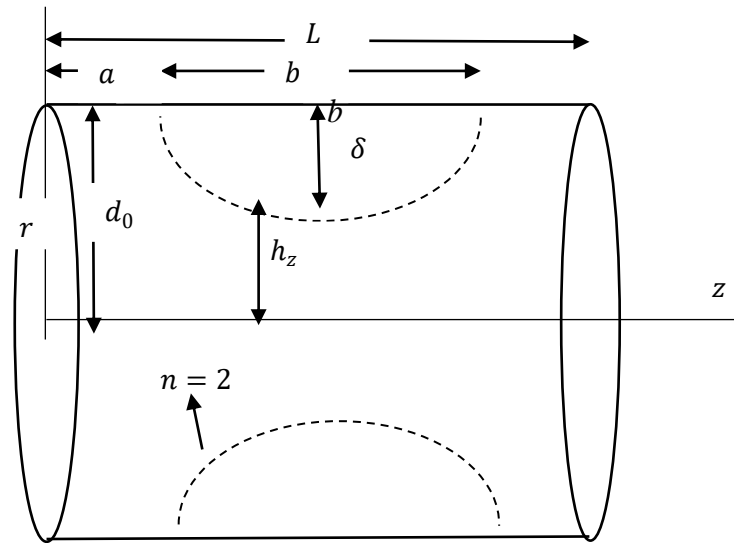
Fig. 1. Schematic diagram of stenotic artery with coordinate system.

For non-tapered artery $\tilde{\theta} = 0$, divergent artery $\tilde{\theta} \geq 0$ and convergent artery $\tilde{\theta} \leq 0$. Further, following conditions are also used to consider mild stenosis:

$$\frac{\delta}{d_0} \ll 1 \; ; \; \frac{Re\delta n^{\left(\frac{1}{n-1}\right)}}{b} \ll 1 \; ; \; \frac{d_0 n^{\left(\frac{1}{n-1}\right)}}{b} \sim 0 \; .$$

The equations governing steady flow of incompressible Reiner – Rivlin in cylindrical coordinate considering suitable transformation for non-dimensional parameters and mild stenosis conditions reduce to [27, 28]:

$$\frac{\partial u}{\partial r} + \frac{u}{r} + \frac{\partial w}{\partial z} = 0 \tag{2}$$

$$\frac{\partial p}{\partial r} = 0 \tag{3}$$

$$\frac{\partial p}{\partial z} = \frac{1}{r} \frac{\partial}{\partial r} \left[r \frac{\partial w}{\partial r} + 2\beta r \frac{\partial w}{\partial r} \frac{\partial w}{\partial z} \right] \tag{4}$$

SOLUTION OF PROBLEM

closed-form solution for velocity is obtained from Eq. (4) considering the boundary and initial condition as: $\dfrac{\partial w}{\partial r} = 0$ at $r = 0$; $w = 0$ at $r = h_z$ and $u =$ finite and constant:

$$w = \frac{1}{2} \frac{\partial p}{\partial z} \left[\frac{r^2}{2} + 2\beta u r + 2\beta^2 u^2 ln (r - 2\beta u)^2 \right] + C \; , \tag{5}$$

where C is constant of integration to be evaluated by using following boundary conditions. At $r = h_z$, $w = 0$, equation (5) becomes:

$$w = \frac{1}{2} \frac{\partial p}{\partial z}\left[\frac{r^2 - h_z^2}{2} + 2\beta u\left(r - h_z\right) + 2\beta^2 u^2 ln\left(\frac{r - 2\beta u}{h_z - 2\beta u}\right)^2\right]. \tag{6}$$

The volume flow rate being initial condition is utilized to obtain axial pressure gradient ($\frac{\partial p}{\partial z}$) from [27, 28].

Substituting Eq. 6 in Volume flow rate, $Q = 2\pi \int\limits_0^{h_z} rwdr$, ($\frac{\partial p}{\partial z}$) is evaluated as:

$$\frac{\partial p}{\partial z} = 4(\beta u)^4 \, ln\left(\frac{2\beta u}{h_z - 2\beta u}\right)^2 - 4\beta^3 u^3 h_z - \beta^2 u^2 h_z^2 - \frac{\beta u h_z^3}{3} - \frac{h_z^4}{8}.$$

Substituting the axial pressure gradient ($\frac{\partial p}{\partial z}$) in Eq. 6 it becomes:

$$w = \frac{Q\left[\left(\dfrac{h_z^2 - r^2}{2}\right) + 2\beta u\left(h_z - r\right) - 2\beta^2 u^2 ln\left(\dfrac{r - 2\beta u}{h_z - 2\beta u}\right)^2\right]}{\pi\left[4(\beta u)^4 \, ln\left(\dfrac{2\beta u}{h_z - 2\beta u}\right)^2 - 4\beta^3 u^3 h_z - \beta^2 u^2 h_z^2 - \dfrac{\beta u h_z^3}{3} - \dfrac{h_z^4}{8}\right]} \tag{7}$$

Resistance impedence [27, 28]:

$$\gamma = \frac{\Delta p}{Q} = \int\limits_0^s \left(-\frac{\partial p}{\partial z}\right)dz + \int\limits_s^{s+1}\left(-\frac{\partial p}{\partial z}\right)dz + \int\limits_{s+1}^{2s+1}\left(-\frac{\partial p}{\partial z}\right)dz \ , \tag{8}$$

where $\Delta p = \int\limits_0^{2s+1}\left(-\frac{\partial p}{\partial z}\right)dz$.

Wall shear stress [27, 28]:

$$\tau_{rz} = \left\{\frac{\partial w}{\partial r} - 2\beta\frac{\partial w}{\partial r}\left(\frac{u}{r}\right)|r = h_z\right\}.$$

Then, using Equation (7) in above relation wall shear stress can be expresses as:

$$\tau_{rz} = \frac{Qh_z^2}{\left(2\beta u - h_z\right)\left[\dfrac{h_z^4}{8} + \dfrac{\beta u h_z^3}{3} + \dfrac{\beta^2 u^2 h_z^2}{2} + 4\beta^3 u^3 h_z + 4(\beta u)^4 \, ln\left(\dfrac{2\beta u - h_z}{2\beta u}\right)^2\right]}. \tag{9}$$

The effect of viscosity, flow rate, degree of stenosis and type of tapered artery on velocity, resistance impedence and wall shear stress are studied by using Equations 7, 8 and 9 respectively.

NUMERICAL RESULTS AND DISCUSSION

The computer codes are written in MATLAB to compute the velocity, resistance impedence and wall shear stress to study its variation with respect to different parameters such as ratio of cross viscosity to viscosity, flow rate, amount of stenosis for three different types of artery namely non-tapered, convergent and divergent.

From Eq. 1, it is seen that the radius of artery at any axial length depends on height of stenosis, taper angle of artery and shape factor. A MATLAB code for Eq. 1 is written to

300

calculate the radius of artery and the longitudinal sectional view of stenotic artery for different shape parameter, taper angle of artery and height of stenosis are shown in Fig. 1, Fig. 3, Fig. 5 and Fig. 7 respectively. Few wireframe views in Fig. 3, Fig. 5, Fig. 7 and Fig. 9 are developed in CAD-CAE software by revolving the longitudinal sectional surface obtained from Eq. 1 for different shape parameter, taper angle of artery and height of stenosis. In CAD software, a surface is drawn corresponding to the longitudinal cross section and the by the surface revolution menu the surface is rotated to obtain a 3 D view of the stenotic artery. The wireframe view exhibits a clear view of the stenotic artery for different shape parameter, taper angle of artery and height of stenosis.

Fig. 2 and Fig. 3 show the effect of shape parameter for non-tapered artery considering $\delta = 0.25$ that implies the artery is 25 % clogged. For shape parameter $(n=2)$, the stenosis is symmetric and location of maximum constriction is at middle of stenotic length. It is observed that as the value of shape parameter (n) increases, the location of maximum constriction shift towards right.
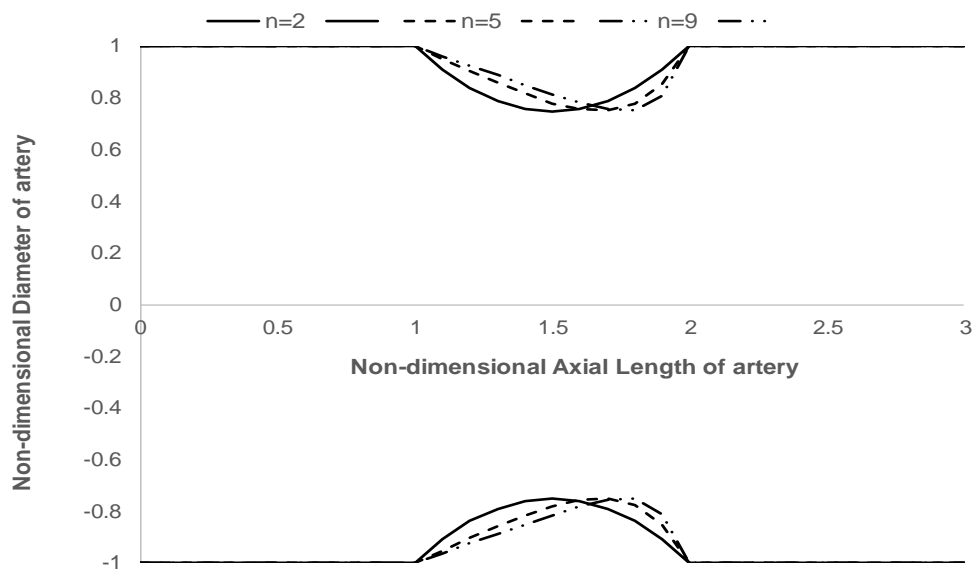
Fig. 2. Shape of stenosis at different shape parameter (*n*) for non-tapered artery, δ = 0.25, *s* = 1.

Shape factor: *n* = 2   Shape factor: *n* = 5   Shape factor: *n* = 9
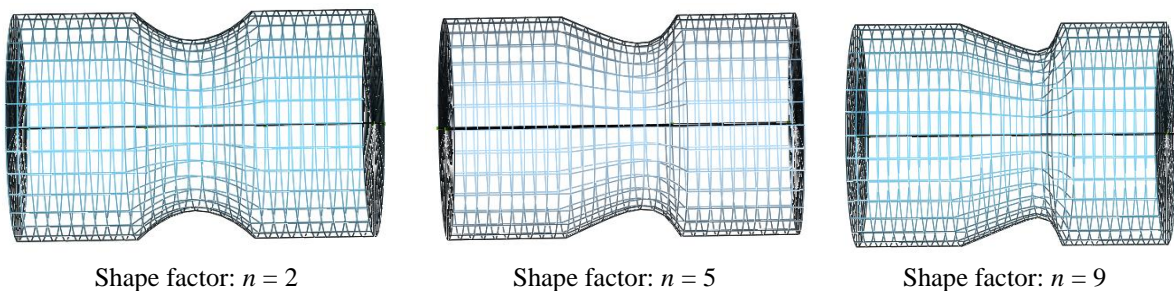
Fig. 3. Wireframe view of shape of stenosis at different shape parameter (*n*) for non-tapered artery, δ = 0.25, *s* = 1.

301

Fig. 4. Shape of stenosis at different shape parameter (n) for divergent artery, $\delta = 0.25$, $s = 1$, $\theta = 25^0$.

Shape factor: $n = 2$ Shape factor: $n = 5$ Shape factor: $n = 9$
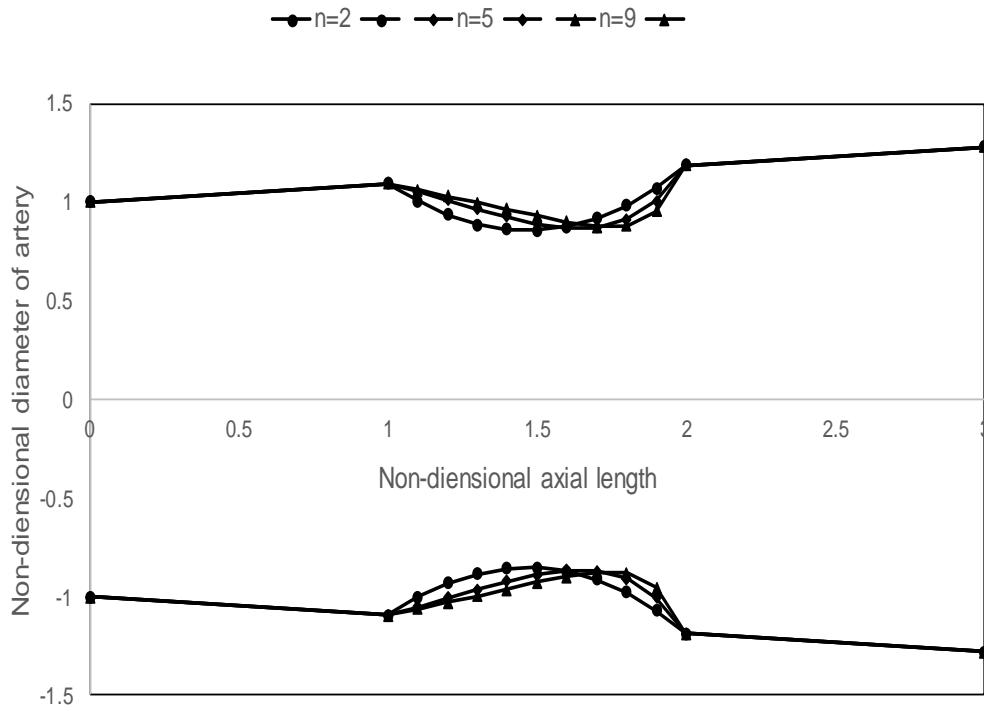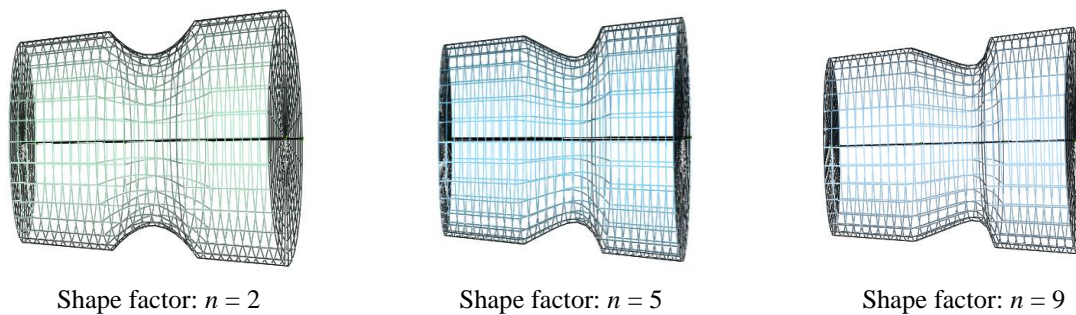
Fig. 5. Wireframe view of shape of stenosis at different shape parameter (n) for divergent artery, $\delta = 0.25$, $s = 1$, $\theta = 25^0$.

The effect of tapered artery is shown from Fig. 4 to Fig. 7. The divergent artery shown in Fig. 4 and Fig. 5 expands rightward by a positive taper angle. As the length of artery increases the cross section of artery also gradually increases. The effect of shape parameter on divergent artery is seen on Fig. 5.

The convergent artery in Fig. 6 and Fig. 7 show gradual reduction in cross sectional area of artery along axial length by a negative taper angle and eventually, the longitudinal symmetry is lost. It is observed that the tapering of artery and shape parameter alter the longitudinal symmetry of artery under stenotic length.

The effect of tapered artery at a particular shape parameter ($n = 2$) has been plotted in Fig. 8 and Fig. 9. It exhibits that maximum constriction and its location is effected by variation in taper angle.

The location of maximum constriction has been determined at different shape parameter for $\left(\theta = -15^0\right)$ convergent, non-tapered and $\left(\theta = +15^0\right)$ divergent artery and is plotted in Fig. 10. From Fig. 10, it may be concluded that both shape factor and taper angle of artery influences the location of maximum stenotic constriction along axial length of artery. Thus, in turn, both

302

shape factor and taper angle of artery is expected to affect the velocity of flow of Reiner – Rivlin flow of blood in stenotic artery.
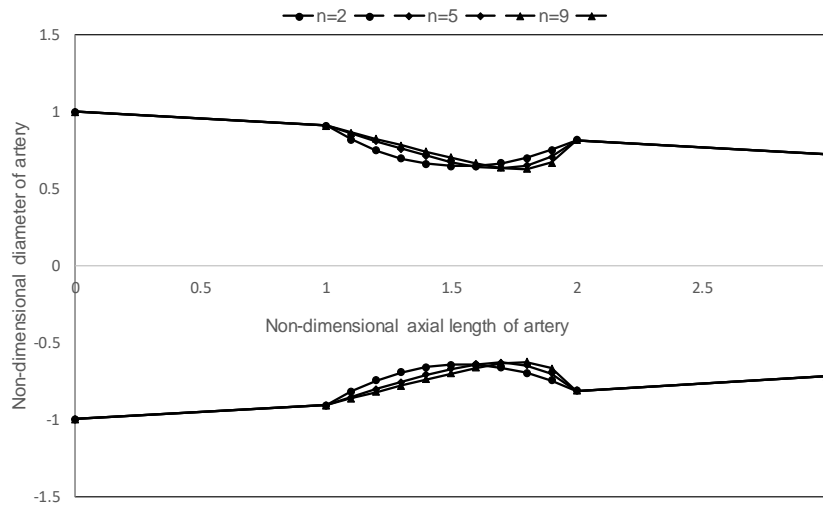
Fig. 6. Shape of stenosis at different shape parameter (n) for convergent artery, $\delta = 0.25$, $s = 1$, $\theta = -25^0$.

Shape factor: $n = 2$ Shape factor: $n = 5$ Shape factor: $n = 9$
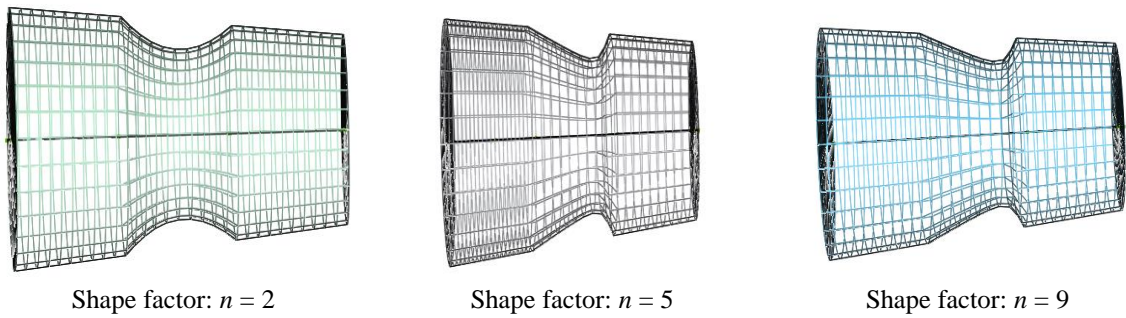
Fig. 7. Wireframe view of shape of stenosis at different shape parameter (n) for convergent artery, $\delta = 0.25$, $s = 1$, $\theta = -25^0$.
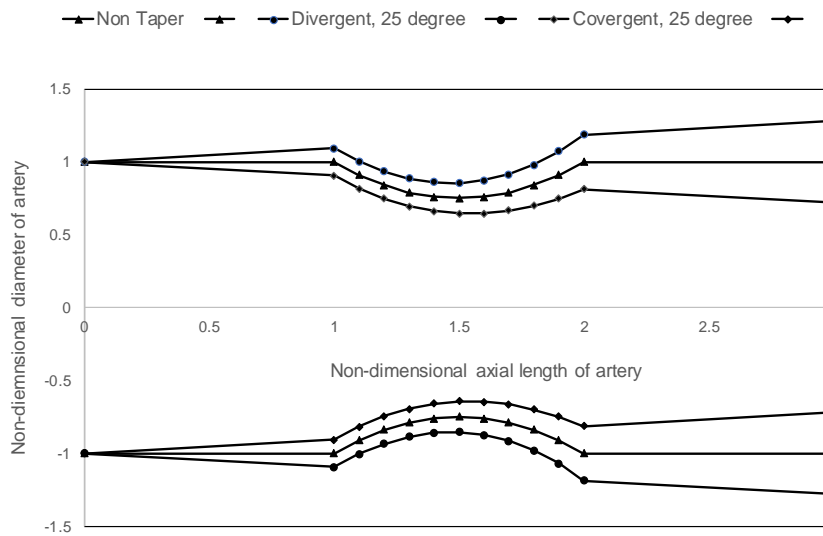
Fig. 8. Shape of tapered artery with symmetric stenosis, $n = 2$, $\delta = 0.25$, $s = 1$.

303

Non-tapered artery ($\theta = 0^0$)   Divergent artery ($\theta = 25^0$)   Convergent artery ($\theta = 25^0$)
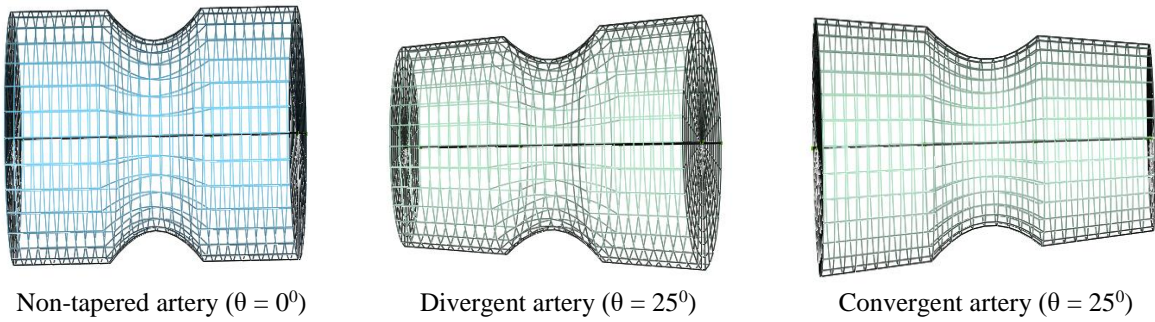
Fig. 9. Wireframe view of shape of stenosis for non-tapered, divergent and convergent artery, $n = 2$, $\delta = 0.25$, $s = 1$.
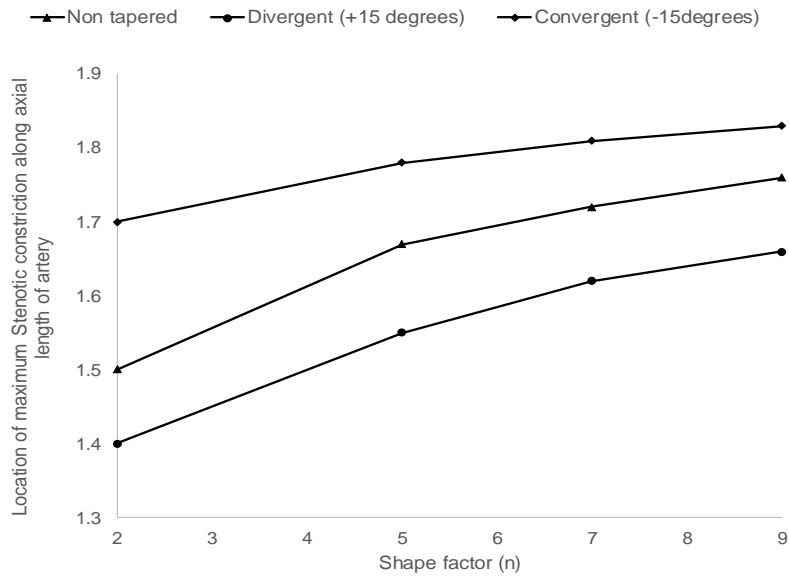
Fig. 10. Effect of shape factor and taper angle on location of maximum stenotic constriction along axial length of artery, $\delta = 0.25$, $s = 1$.
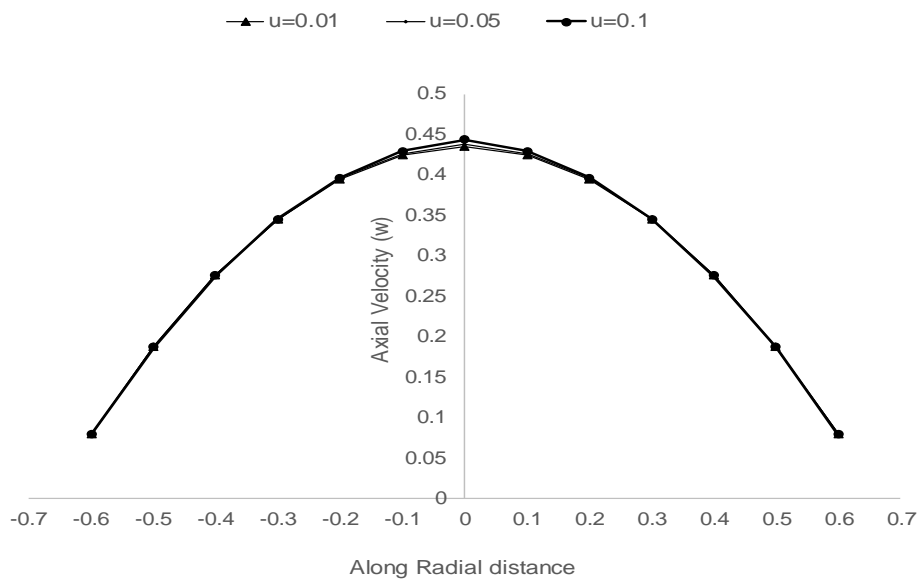
Fig. 11. Variation of axial velocity with respect to radial distance in non-tapered artery at different radial velocity u, $n = 2$, $\delta = 0.25$, $s = 1$, $z = 1.1$, $Q = 0.3$ and $\beta = 0.1$.

304

The axial velocity component can be computed from Equation 7 by considering suitable values of radial velocity (u), volume flow rate (Q), non-dimensional ratio of cross viscosity to viscosity (β), non-dimensional radius of artery (h_z). First few graph are plotted to study the effect of variation of these parameters on axial component of velocity. The effect of radial velocity on axial velocity profile of non-tapered artery has been shown in Fig. 11.

It is observed that change in radial velocity has a little effect on axial velocity profile. The variation in (u) does not affect the axial velocity profile along arterial wall. Therefore, the value of (u) is kept fixed at 0.01 for further study of the effect of other parameters on axial velocity profile.
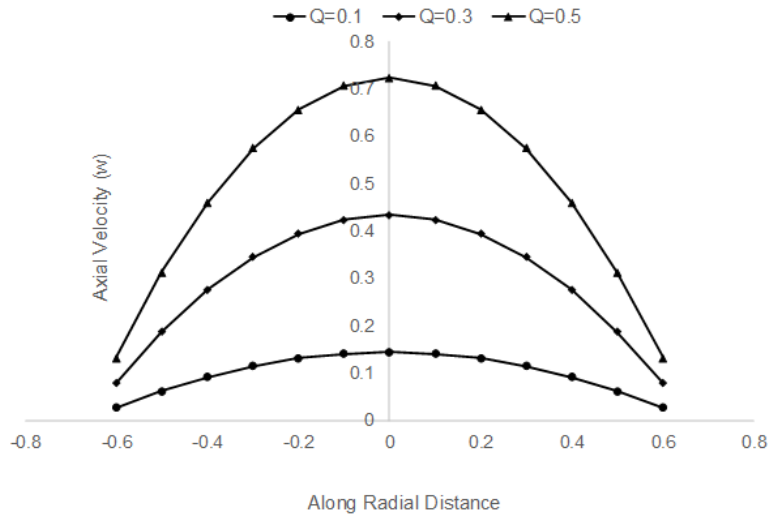
Fig. 12. Variation of axial velocity profile with respect to radial distance in non-tapered artery at different volumetric flow rate Q, n =2, δ = 0.4, s = 1, z = 1.3, u = 0.01 and β = 0.1.

The axial velocity profile with respect to radial distance at different volumetric flow rate has been plotted in Fig. 12. It is observed that higher flow rate provides larger axial velocity profile across the cross section of artery.
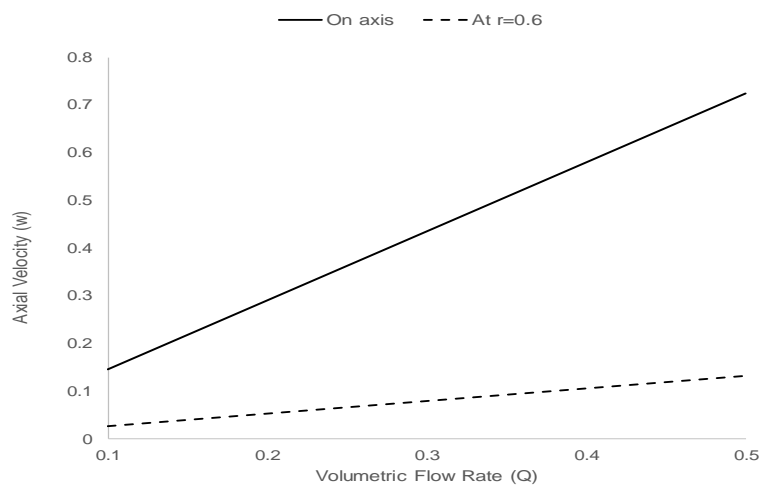
Fig. 13. Effect of volumetric flow rate (Q) on axial velocity profile in non-tapered artery, n =2, δ = 0.4, s = 1, z = 0.3, u = 0.01 and β = 0.1.

305
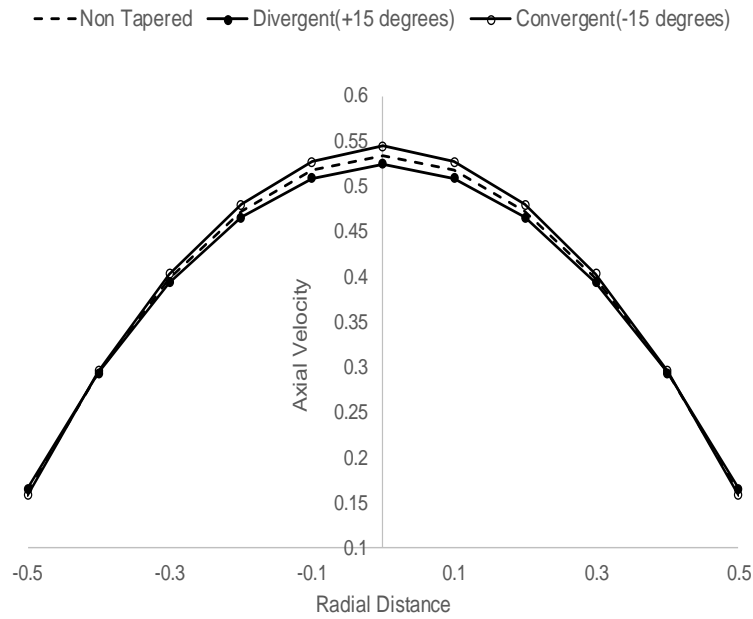
Fig. 14. Variation of axial velocity profile with respect to radial distance for non-tapered, divergent and convergent artery, $n = 2$, $\delta = 0.4$, $s = 0$, $z = 0.5$, $Q = 0.3$, $u = 0.01$ and $\beta = 0.3$.
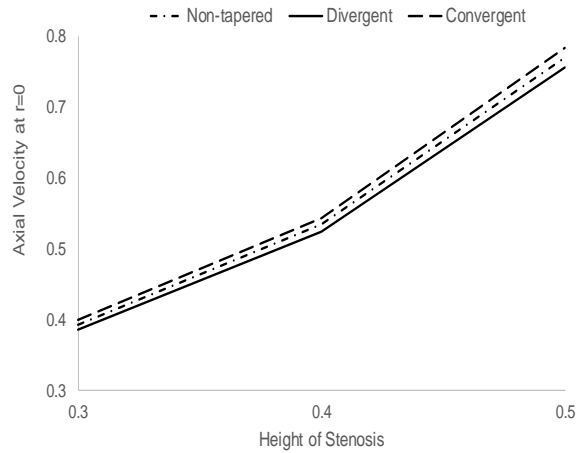
Fig. 15. Variation of axial velocity for non-tapered, divergent and convergent artery with respect to height of stenosis δ, $s = 0$, $r = 0$, $z = 0.5$, $Q = 0.3$, $u = 0.01$, $\beta = 0.3$, $n = 2$.
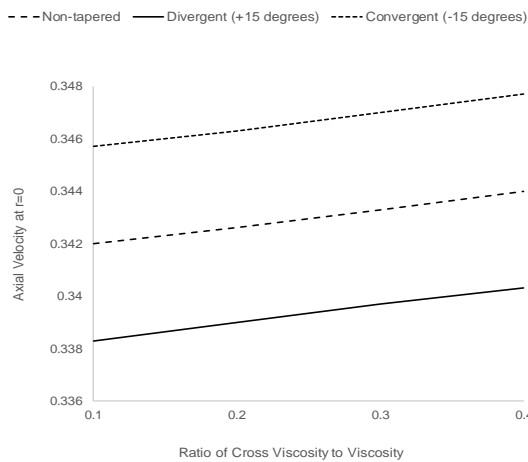
Fig. 16. Variation of axial velocity for non-tapered, divergent and convergent artery with respect to ratio of cross-viscosity to viscosity β, $n = 2$, $s = 0$, $r = 0$, $z = 0.5$, $Q = 0.3$, $u = 0.01$, and $\delta = 0.4$.
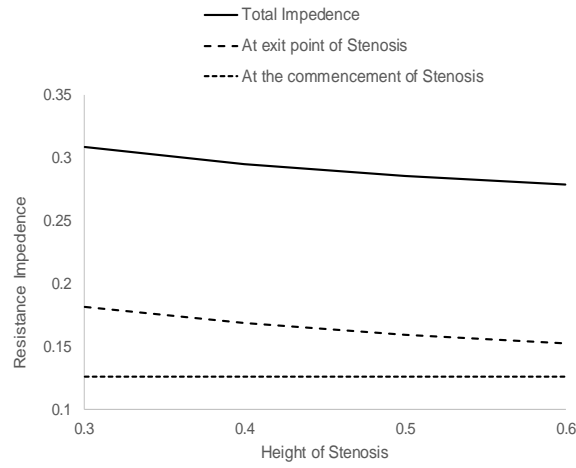
Fig. 17. Variation of resistance impedence with respect to height of stenosis for non-tapered artery, $n = 2$, $s = 1$, $L = 2s + 1$, $Q = 0.3$, $u = 0.01$ and $\beta = 0.3$.
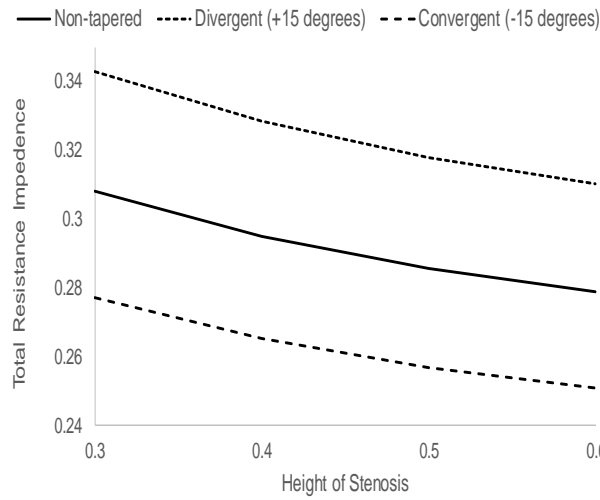
Fig. 18. Variation of total resistance impedence with respect to height of stenosis for non-tapered, divergent and convergent artery, $n = 2$, $s = 1$, $L = 2s + 1$, $Q = 0.3$, $u = 0.01$ and $\beta = 0.3$.
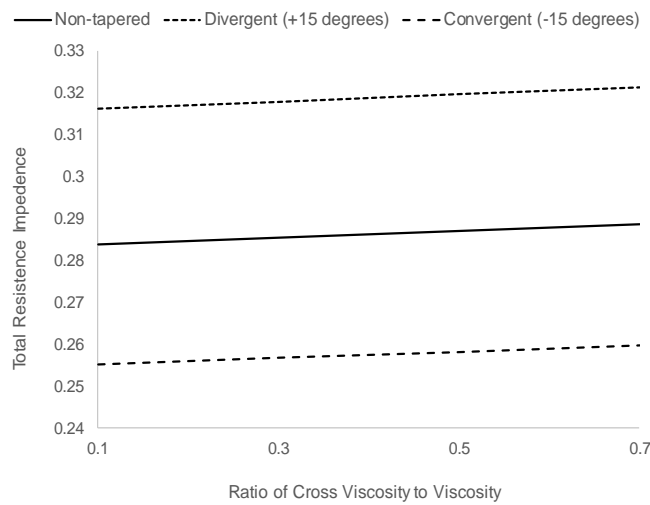
Fig. 19. Variation of total resistance impedence for non-tapered, divergent and convergent artery with respect to ratio of cross-viscosity to viscosity β, $n = 2$, $s = 0$, $L = 2s + 1$, $Q = 0.3$, $u = 0.01$ and $\delta = 0.5$.

307
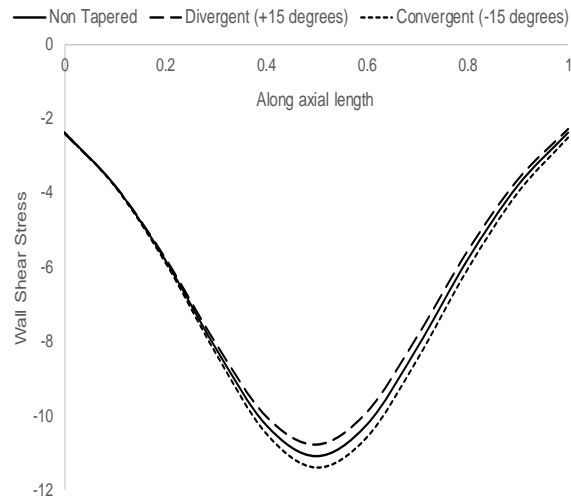
Fig. 20. Variation of wall shear stress with respect to axial length in non-tapered, divergent and convergent artery, $n = 2$, $s = 0$, $\delta = 0.4$, $Q = 0.3$, $u = 0.1$ and $\beta = 0.1$.
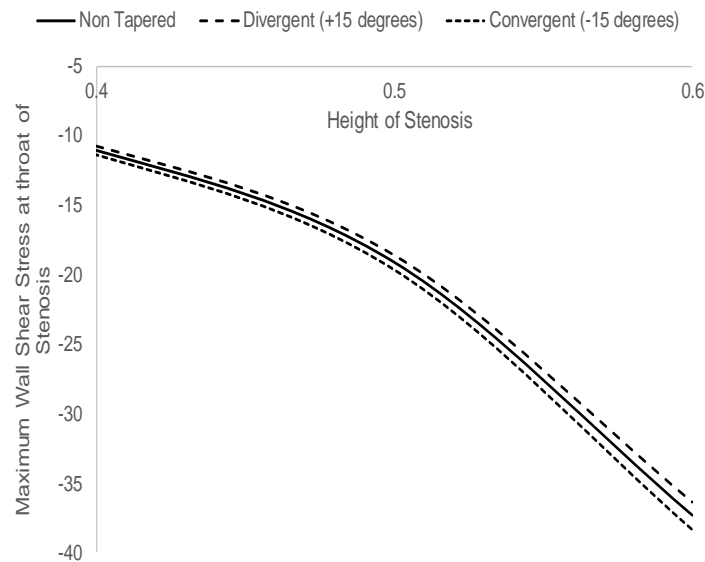
Fig. 21. Variation of maximum wall shear stress at throat of stenosis with respect to height of stenosis for non-tapered, divergent and convergent artery, $n = 2$, $s = 0$, $\delta = 0.4$, $Q = 0.3$, $u = 0.1$ and $\beta = 0.3$.
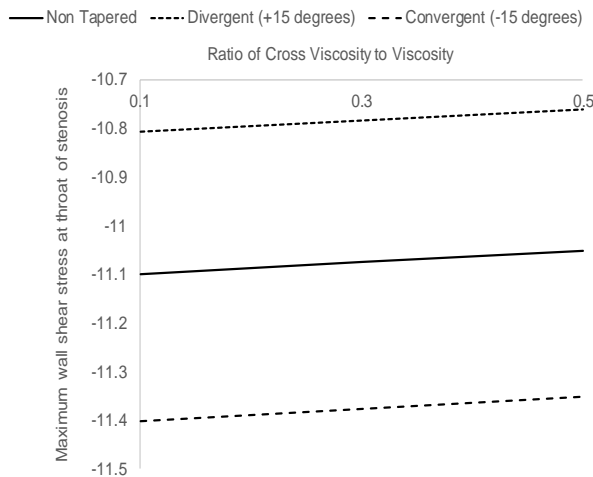
Fig. 22. Variation of maximum wall shear stress at throat of stenosis with respect to ratio of cross-viscosity to viscosity for non-tapered, divergent and convergent artery, $n = 2$, $s = 0$, $Q = 0.3$, $u = 0.1$ and $\delta = 0.4$.

308
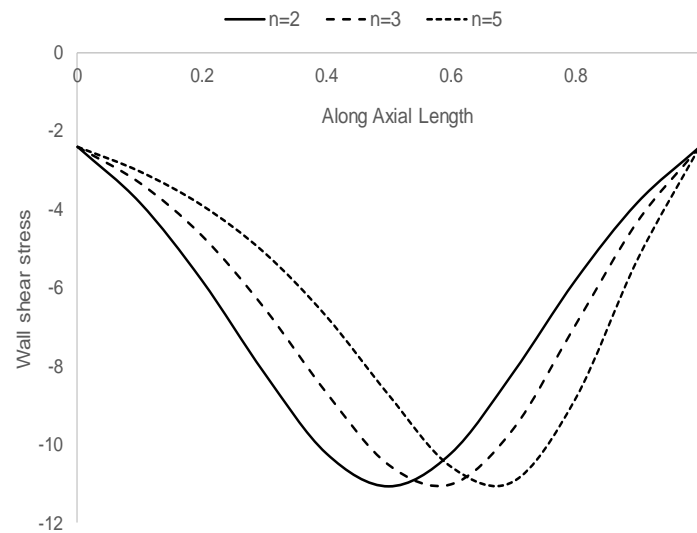
Fig. 23. Variation of wall shear stress with respect to axial length for different shape factor in non-tapered artery, $s = 0$, $\delta = 0.4$, $Q = 0.3$, $u = 0.1$ and $\beta = 0.3$.

In Fig. 13, the variation of axial velocity with respect to volumetric flow rate has been plotted. With the increase in volumetric flow rate, axial velocity increases linearly. But, the rate of increase of axial velocity shows a decreasing trend as it moves away from axis. Considering the linear relationship with respect to volumetric flow rate, the value of volumetric velocity is kept fixed at 0.3 for further study.

Fig. 14 shows the axial velocity profile across cross section of artery for non-tapered, divergent and convergent artery. The trend shows similarity to the earlier reported trend [27, 28].

In Fig. 15, the effect of stenosis height (δ) on axial velocity at the longitudinal axis has been shown. It is inferred from Fig. 15 that axial velocity is non-linearly related to height of stenosis and trend of evolution of axial velocity is similar in non-tapered, divergent and convergent artery. The effect of variation of ratio of cross viscosity to viscosity (β) on axial velocity at the centre of artery is shown in Fig. 16. It is seen that the effect of increase in (β) is linear on axial velocity and causes same nature of effect in non-tapered and tapered artery but differs by magnitude.

Resistance impedence is calculated numerically from Equation 8. In Fig. 17, the effect of height of stenosis on impedence at the commencement of stenosis and at the end of stenosis and total stenosis considering equal length before and after stenosis of artery are plotted. It is observed that higher the height of stenosis lowers the value of impedence. The variation of impedence with respect to height of stenosis for non-tapered and tapered artery shown in Fig. 18 and with respect to ratio of cross viscosity to viscosity in Fig. 19 show similar trend line reported in earlier literature [28].

Wall shear stress at any axial length (z) is computed from Equation 9, considering $r = h_z$. The variation of wall shear stress across the length of the artery under the stenotic region is plotted in Fig. 20. It is found that in the upstream the wall shear stress decreases steeply from the value at its approach to a peak value at the at the throat of the stenosis where the cross section of artery gets reduced to minimum due the onset of stenosis. Beyond this in the downstream again it increases steeply to regain its approach value. As the blood enters into stenotic region, it tends to develop higher wall shear stress. The magnitude of wall shear stress at the commencement of stenosis region shows no remarkable difference in tapered and non-

tapered artery. But, gradually the profile of wall shear stress with respect to axial length starts differentiating. The difference is maximum at the throat of the stenosis, where the cross section of artery is minimum. Further, it is determined that for a divergent artery, the magnitude of stress evolved is higher than in the order of non-tapered and convergent artery. The effect of height of stenosis on maximum wall shear stress at the throat of the stenosis is computed and plotted in Fig. 21. It is inferred that the height of stenosis significantly affects the evolution of peak wall shear stress. Therefore, greater the degree of constriction higher is the magnitude of difference in peak wall shear stress in comparison to wall shear stress at the approach. The effect of cross viscosity on wall shear stress is shown in Fig. 22, where in it observed that higher the cross viscous value relative to viscous term relatively more wall shear stress is generated at the throat of the stenosis. However, the effect is found to be linear with a marginal slope and similar trend is found in tapered and non-tapered artery. In Fig. 23, the effect of shape factor (n) on wall shear stress is plotted. From Fig. 23, it is observed that during upstream the rate of decrease of wall shear stress decreases with increase in shape factor (n). But in the downstream of the throat, the rate of increase of wall shear stress significantly increase with the increase in shape factor (n). Similar conclusions are reported by Mekheimer and Kot [27], Akbar et al. [28] and Srivastava [31].

CONCLUSION

A mathematical model for axisymmetric blood flow through an axially non-symmetric but radially symmetric mild stenosis in a tapered artery is worked out. Blood flow is considered to obey Reiner – Rivlin fluid having an additional cross viscosity parameter. The exact expressions for the axial velocity, volume flow rate, resistance impedance, wall shear stress distribution in the stenotic region and its magnitude at the stenosis throat are derived by solving continuity and momentum equations. The nature of variation with respect to different parameters are studied by plotting graphs of the results. The main findings can be summarized as follows:

i.   Tapered artery of a particular taper angle and shape factor individually and jointly defines the location of throat of stenotic constriction and the height of stenosis. Both in turn, influence the fluid flow pattern.

ii.   The flow pattern is significantly dependent on volumetric flow rate and value of cross viscosity relative to viscosity and is non-linearly related to height of stenosis.

iii.   Impedence increases with the increase in the value of cross viscosity relative to viscosity.

iv.   For a divergent artery, the magnitude of wall shear stress evolved is higher than in the order of non-tapered and convergent artery.

v.   Height of stenosis significantly affects the evolution of peak wall shear stress.

vi.   Higher the cross viscous value relative to viscous term relatively more wall shear stress is generated at the throat of the stenosis.

vii.   Shape factor and taper angle significantly affect the rate of decrease and increase of wall shear stress in upstream and downstream respectively.

NOMENCLATURE

u : Non-dimensional Radial Component of velocity of flow

$\bar{u}$: Radial Component of velocity of flow [ms^{-1}]

u_0 : Averaged velocity on cross section of artery [ms^{-1}]

w : Non-dimensional Axial Component of velocity of flow

$\bar{w}$: Axial Component of velocity of flow [ms^{-1}]

p : Non-dimensional Pressure

310

$\bar{p}$: Arterial Pressure [Nm^{-2}]

β : Ratio of cross-viscosity to viscosity

Re : Reynold number

a : Length of artery before the commencement of stenosis [m]

b : Length of artery in stenotic region [m]

L : Total length of artery [m]

δ : Maximum height of stenosis [m]

d_z : Radius of the tapered arterial segment

d_0 : Radius of non-tapered artery in non-stenotic region [m]

$\tilde{\theta}$: Tapered angle of artery, [rad]

ρ : Density of blood [kg m^{-3}]

t : Non-dimensional time

r : Non-dimensional radial distance

z : Non-dimensional axial distance

θ : Non-dimensional angular distance

μ : Coefficient of Newtonian viscosity [kg m^{-1}s^{-1}]

μ_c : Coefficient of Cross Viscosity [ms^{-1}].

REFERENCES

1. Lim S.S., Vos T. A comparative risk assessment of burden of disease and injury attributable to 67 risk factors and risk factor clusters in 21 regions, 1990–2010: A systematic analysis for the Global Burden of Disease Study 2010. *The Lancet*. 2012. V. 380. P. 2224–2260.

2. Young D.F. Fluid mechanics of arterial stenosis. *J. Biomech. Eng*. 1979. V. 101. P. 157–175.

3. Young D.F. Effect of a time-dependent stenosis on flow through a tube. *J. Manuf. Sci. Eng*. 1968. V. 90. P. 248–254.

4. Young D.F., Tsai F.Y. Flow characteristics in models of arterial stenosis I. Steady flow. *J Biomech*. 1973. V. 6. P. 395–402.

5. Padmanabhan N. Mathematical model of arterial stenosis. *Med. Biol. Eng. Comput*. 1980. V. 18. P. 281–286.

6. Sapna S. Analysis of non-Newtonian fluid flow in a stenosed artery. *Int. J. Phys. Sci*. 2009. V. 4. № 11. P. 663–671.

7. Cokelet G.R., Merrill E.W., Gilliland E.R., Singh H. The Rheology of Human Blood Measurement near and at Zero Shear Rate. *Trans. Soc. Rheol*. 1963. V. 7. P. 303–317.

8. Goldsmith H.L., Skalak R. Hemodynamics In: Annual Review of Fluid Dynamics. *Annual Review Inc. Pato. Alto. Pub*. 1975. P. 231–247.

9. Smith N.P., Pullan A.J., Hunter P.J. An Anatomically Based Mode for Transient Coronary Blood Flow in the Heart. *SIAM J. Appl. Math*. 2002. V. 62. № 3. P. 990–1018.

10. Anastasiou A.D., Spyrogianni A.S., Koskinas K.C., Giannoglou G.D., Paras S.V. Experimental investigation of the flow of a blood analogue fluid in a replica of a bifurcated small artery. *Medical Engineering & Physics*. 2012. V. 34. P. 211–218.

11. Yilmaz F., Gundogdu M.Y. A critical review on blood flow in large arteries; relevance to blood rheology, viscosity models, and physiologic conditions. *Korea-Australia Rheology Journal*. 2008. V. 20. № 4. P. 197–211.

12. Mekheimer Kh.S., El Kot M.A. Mathematical modelling of unsteady flow of a Sisko fluid through an anisotropically tapered elastic arteries with time-variant overlapping stenosis. *Applied Mathematical Modelling*. 2012. V. 36. P. 5393–5407.

13. Antonova N. On Some Mathematical Models in Hemorheology. *Biotechnology & Biotechnological Equipment*. 2012. V. 26. № 5. P. 3286–3291.
14. Thomas B., Suman K.S. Blood Flow in Human Arterial System-A Review. *Procedia Technology*. 2016. V. 24. P. 339–346.
15. Verma V.K. Study of Non-Newtonian Herschel-Bulkley Model through Stenosed Arteries. *International Journal of Mathematics and its Applications*. 2016. V. 4. P. 105–111.
16. Jahangiri M., Saghafian M., Sadeghi M.R. Effect of six non-Newtonian viscosity models on hemodynamic parameters of pulsatile blood flow in stenosed artery. *Jl. of Computational and Applied Research in Mechanical Engineering*. 2018. V. 29. № 7. P. 199–207.
17. Tu C., Deville M. Pulsatile flow of non-Newtonian fluids through arterial stenoses. *Journal of Biomechanics*. 1996. l. 29. № 7. P. 899–908.
18. Sankar D.S., Yatim Y. Comparative Analysis of Mathematical Models for Blood Flow in Tapered Constricted Arteries. *Abstract and Applied Analysis*. 2012. Article ID 235960.
19. Tesch K. Generalised Herschel model applied to blood flow modelling. *Task Quarterly*. 2012. V. 16. № 3–4. P. 253–262.
20. Verma V.K. Study of Non-Newtonian Herschel-Bulkley Model through Stenosed Arteries. *International Journal of Mathematics and its application*. 2016. V. 4. № 1-B. P. 105–111.
21. Iida N. Influence of plasma layer on steady blood flow in micro vessels. *Japanese Journal of Applied Physics*. 1978. V. 17. P. 203–214.
22. Chaturani P., Palanisamy V. Casson fluid model for pulsatile flow of blood under periodic body acceleration. *Biorheology*. 1990. V. 27. № 5. P. 619–630.
23. O'Callaghan S., Walsh M., McGloughlin T. Numerical modelling of Newtonian and non-Newtonian representation of blood in a distal end-to-side vascular bypass graft anastomosis. *Med. Eng. Phys.* 2006. V. 28. P. 70–74.
24. Hall P. Viscous flow in a pipe of slowly varying crosssection. *J. Fluid Mech.* 1974. V. 64. P. 209–226.
25. Porenta G., Young G.F., Rogge T.R. A finite element model of blood flow in arteries including taper, branches and obstructions. *J. Biomech. Eng.* 1986. V. 108. P. 161–167.
26. Greensmith H.W., Rivlin R.S. The Hydrodynamics of non-Newtonian fluids III. Theoretical stress effect in polymer solutions. *Phil. Trans. Roy. Soc. London*. 1953. V. 245. P. 399.
27. Mekheimer Kh.S., El Kot M.A. The micropolar fluid model for blood flow through a tapered artery with a stenosis. *Acta Mech. Sin.* 2008. V. 24. P. 637–644.
28. Akbar N.S., Nadeem S., Mekheimer Kh.S. Rheological properties of Reiner – Rivlin fluid model for blood flow through tapered artery with stenosis. *Journal of the Egyptian Mathematical Society*. 2016. V. 24. P. 138–142.
29. Rathna S.L., Bhatnagar P.L. Weissenberg and Merrington effects in non-newtonian fluids. *Jl. of Indian Institute of Science*. 1962. V. 45. № 3. P. 57–82.
30. Narasimham M.N.L. On steady laminar flow of certain non-Newtonian liquids through an elastic tube. *Proceedings of Indian Academy of Sciences*. 1956. V. 43. № 4. P. 237–246.
31. Srivastava V.P. Arterial blood flow through a nonsymmetrical stenosis with applications. *Jpn. J. Appl. Phys.* 1995. V. 34. P. 6539–6545.